Semicond. Sci. Technol. 19 (2004) 461–467 PII: S0268-1242(04)69089-4

Electrical transport and low frequency noise characteristics of Au/n-GaAs Schottky diodes containing InAs quantum dots

N A Hastas[1], D H Tassis[1], C A Dimitriadis[1], L Dozsa[2], S Franchi[3] and P Frigeri[3]

[1] Department of Physics, University of Thessaloniki, 54124 Thessaloniki, Greece
[2] Hungarian Academy of Sciences, Research Institute for Technical Physics and Materials Science, PO Box 49, Budapest 114, H-1525, Hungary
[3] IMEM Institute, CNR, Parco Area dele Scienze, 43010 Fontanini, Parma, Italy

Received 18 September 2003
Published 13 January 2004
Online at stacks.iop.org/SST/19/461 (DOI: 10.1088/0268-1242/19/3/030)

Abstract
Au/n-GaAs Schottky diodes, containing layers of InAs quantum dots (QDs), are investigated by measuring the forward current–voltage characteristics in the temperature range of 77–300 K and low frequency noise at room temperature. The zero-bias barrier height decreases and the ideality factor increases with decreasing temperature, and the ideality factor was found to follow the T_0-effect. The departure from the ideal thermionic-emission diffusion model was interpreted in terms of inhomogeneous Schottky contact with a Gaussian distribution of barrier heights. The excess current at small biases, observed in diodes containing layers of InAs QDs, was attributed to small patches of reduced barrier height. In the diode without QDs, the noise intensity S_I shows $1/f$ behaviour and is proportional to I_F^2, which is explained by modulation of the barrier height due to trapping processes in interface states. In diodes containing InAs QDs, S_I shows $1/f^\gamma$ (with $\gamma < 1$) behaviour and is proportional to I_F^2 in the high current range, which is explained by generation of band tail states with exponential energy distribution in the GaAs layer due to the QD formation. In the low current range, S_I increases faster than I_F^2 due to contribution to the noise of patches of reduced barrier height.

1. Introduction

Quantum dots (QDs) have attracted great interest in both theoretical and experimental investigations due to their peculiar optical and electronic properties [1]. Among the different techniques proposed for the fabrication of QDs, self-assembled processes during the epitaxial growth of highly lattice-mismatched materials, such as the Stranski–Krastanov growth mode, have been employed to form relatively homogeneous ensembles of QDs [2–4]. QD systems have been recognized to offer the possibility of creating new electronic devices such as detectors [5], lasers [6, 7] and memories [8, 9]. In view of such applications, it is important to understand the electronic properties of the QDs in order to improve the performance of QD-based devices.

In the last few years the electrical characteristics of InAs QDs, embedded in GaAs confining layers, were investigated using Schottky diodes as test devices [10–14]. The most commonly used methods include capacitance spectroscopy [10–12] and deep level transient capacitance spectroscopy [12, 13]. Recently, it has been established that low frequency noise (LFN) measurements are an effective diagnostic tool to characterize the quality and reliability of electronic devices [15]. The noise properties of forward-biased Schottky diodes can provide information on the location and nature of noise sources, as well as on the properties of traps located at the

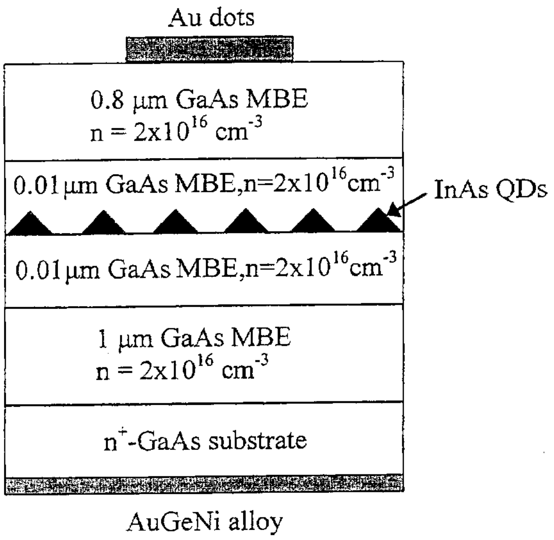

Figure 1. Structure of the investigated Au/n-GaAs Schottky diodes for the sample containing one layer of InAs QDs.

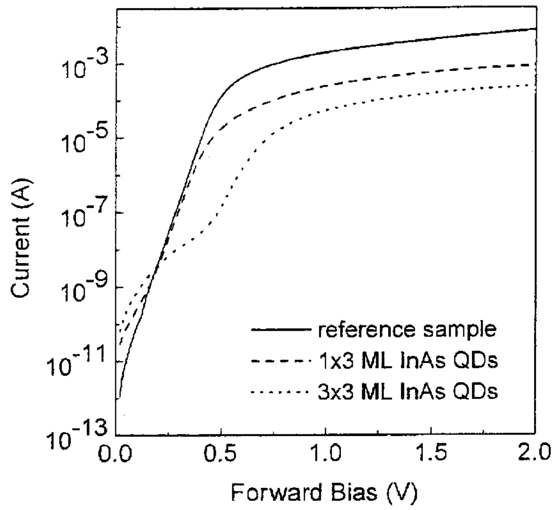

Figure 2. Forward *I–V* characteristics of the three types of Au/n-GaAs Schottky diodes, measured at room temperature.

interface and in the space-charge region of the diode. The trap properties of the GaAs layers, modified after fabrication of the InAs QDs, were studied recently by LFN measurements at room temperature [16, 17].

Although InAs QDs are of great importance in GaAs device technology, details are not available regarding the current transport mechanisms of Au/n-GaAs Schottky diodes over a wide range of temperatures. In the present work, we investigate the current transport characteristics of Au/n-GaAs Schottky diodes containing one or three layers of InAs QDs in the temperature range of 77–300 K. The modifications in the transport mechanisms induced by the QD growth are discussed. We have also utilized the LFN technique to perform electronic characterization of the InAs QD layers, i.e. characterization of the QD growth induced traps in Au/n-GaAs Schottky diodes.

2. Experimental details

The investigated devices are GaAs Schottky diodes with a layer structure shown in figure 1, differing only regarding the insertion of InAs QDs. First, GaAs buffer layers with an electron concentration of 2×10^{16} cm^{-3} (1 μm thick) were grown on n$^+$-GaAs substrate by molecular beam epitaxy (MBE) at 580 °C. Then, a layer of undoped GaAs (10 nm thick) was grown by MBE and three monolayers (3 ML) of InAs QDs were grown by atomic layer MBE (ALMBE) at 460 °C, followed by deposition of another undoped layer of GaAs. Finally, an upper n-GaAs confining layer with an electron concentration of 2×10^{16} cm^{-3} (0.8 μm thick) was grown by MBE at 460 °C. The QD density was found to be about 10^{11} cm^{-2} [18]. We have fabricated three types of samples, one with a layer of InAs QDs, one with three layers of InAs QDs and a sample without InAs, used as a reference sample, for comparison with the InAs QD structures. After the growth of the GaAs layers and the InAs QDs, backside ohmic contacts were formed by evaporation and annealing of the AuGeNi alloy. Schottky diodes were made on the front side of the samples by evaporating circular dots of Au of diameter 400 μm using conventional photolithographic techniques.

The current–voltage (*I–V*) characteristics of the diodes were measured in the temperature range of 77–300 K using a computer controlled system, which includes a Keithley 617 electrometer and a Keithley 230 V source. The diodes were mounted on TO-5 headers using silver paste and placed in a temperature controlled probe station which was cooled down to liquid N_2. The temperature variation was about ±2 K during the measurement at each temperature point. LFN measurements were performed at room temperature and in the forward region of operation using an SR760 spectrum analyser. The current was previously amplified by a low noise current–voltage converter and a low noise voltage amplifier. The bias voltage was supplied from CdNi batteries to avoid any external LFN.

3. Results and discussion

3.1. Current transport characteristics

Typical forward *I–V* semi-log characteristics of the three types of Au/n-GaAs Schottky diodes at room temperature are presented in figure 2. In the reference diode, the plot shows a linearity over six decades of current magnitude with the ideality factor *n* close to 1, suggesting that the thermionic-emission diffusion (TED) theory can be used to model the current in the forward conduction regime. The InAs QDs have a severe effect on the electrical behaviour of the diodes, as they appear to induce larger series resistance compared to the reference diode. The larger decrease of the diode current with increasing number of QD layers is evident due to the larger series resistance induced.

At small biases, an excess current is observed in diodes containing InAs QDs. Generation–recombination in the space-charge region of the contact is the mechanism most frequently thought to lead to the excess current at low biases. If the generation–recombination current dominates at low biases, the ideality factor should be close to 2 and the Richardson plot should give two straight lines [19], which are not our findings.

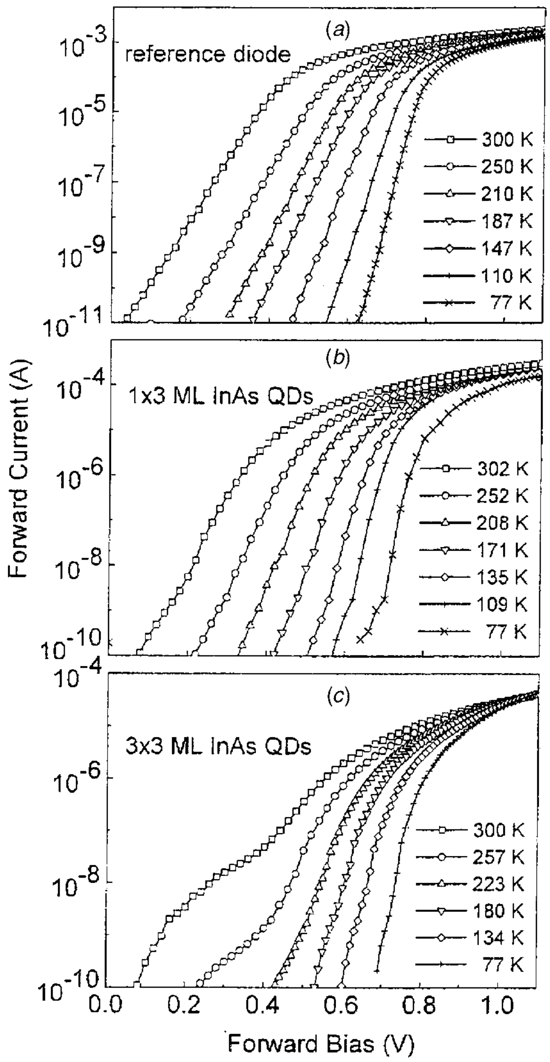

Figure 3. Forward *I–V* characteristics of Au/n-GaAs Schottky diodes at various temperatures fabricated on: (*a*) the reference GaAs sample without containing InAs QDs; (*b*) GaAs containing one layer of InAs QDs and (*c*) GaAs containing three layers of InAs QDs.

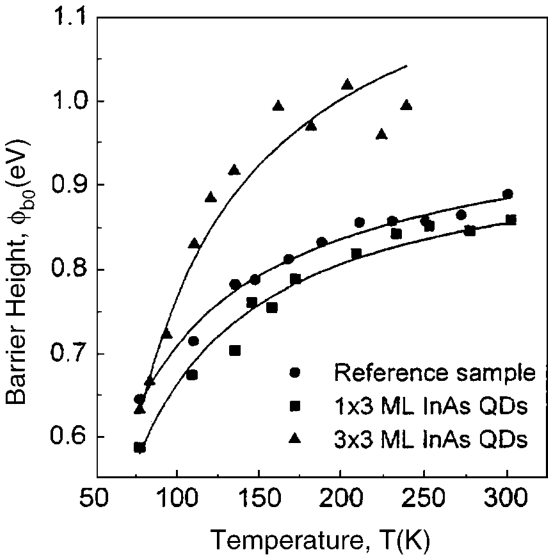

Figure 4. Variation of the zero-bias barrier height with temperature for the three types of Au/n-GaAs Schottky diodes. The experimental data are fitted to equations (5) and (6) (solid lines) using the parameters: (*a*) $\varphi_{b0} = 0.96$ V, $\sigma_0 = 65$ mV for the reference sample; (*b*) $\varphi_{b0} = 0.95$ V, $\sigma_0 = 70$ mV for the sample containing one layer of InAs QDs and (*c*) $\varphi_{b0} = 1.24$ V, $\sigma_0 = 90$ mV for the sample containing three layers of InAs QDs.

Instead of this mechanism, the excess current can be explained by assuming Schottky barrier height (SBH) inhomogeneity. Theoretical simulations have shown that the presence of some small patches of reduced SBH, embedded in the Schottky area, can lead to the appearance of excess current at low bias voltages [20, 21].

For each studied diode, the forward *I–V* characteristics at different temperatures, ranging from 77 to 300 K, are plotted in figure 3. The plots of $\ln I$ versus V clearly show linearity up to six decades of current magnitude. A gradual shift of the *I–V* characteristics towards a higher voltage is observed with decreasing temperature, which is in agreement with the TED equation at forward bias ($V \geqslant 3kT/q$):

$$I = I_s \exp\left(\frac{qV}{nkT}\right) \tag{1}$$

where V is the applied voltage, q is the electronic charge, kT is the thermal energy and I_s is the saturation current defined by

$$I_s = AA^{**}T^2 \exp\left(-\frac{q\varphi_{b0}}{kT}\right) \tag{2}$$

where A is the diode area, A^{**} is the Richardson constant (8.16 A K^{-2} cm^{-2}) and φ_{b0} is the zero-bias Schottky barrier height. The ideality factor n defined as

$$n = \frac{q}{kT}\left(\frac{d\ln I}{dV}\right)^{-1} \tag{3}$$

is introduced to describe the deviation of the experimental *I–V* data from the ideal TED theory.

Using equation (3), the ideality factor n of the diodes at different temperatures was calculated from the slopes of the linear regions of the semi-log *I–V* curves. Using equation (2), the zero-bias barrier height φ_{b0} was determined from the saturation current I_s, obtained from the intercept of the extrapolated linear region with the current axis at $V = 0$. The values of φ_{b0} and n are plotted as a function of temperature in figures 4 and 5, respectively. For the diode containing three layers of QDs, the analysis was restricted to temperatures below 250 K where linear regions in the $\log I$–V characteristics can be clearly seen (figure 3(*c*)). The barrier height decreases whereas the ideality factor increases slowly down to 150 K and then quite rapidly with decreasing temperature down to 77 K. For an ideal Schottky diode, the barrier height should increase as the temperature is decreased, following the band gap variation with temperature [22]. The corresponding Richardson plots, $\ln(I_s/T^2)$ versus $1000/T$, are nonlinear as shown in figure 6 without presenting single activation energy.

The temperature dependence of the ideality factor can reveal the conduction mechanism of a Schottky diode. In Schottky diodes following a non-perfect thermionic-emission model, the ideality factor increases as the temperature decreases, a phenomenon generally known as the T_0-effect [23, 24]. In this approach, the variation of the ideality factor

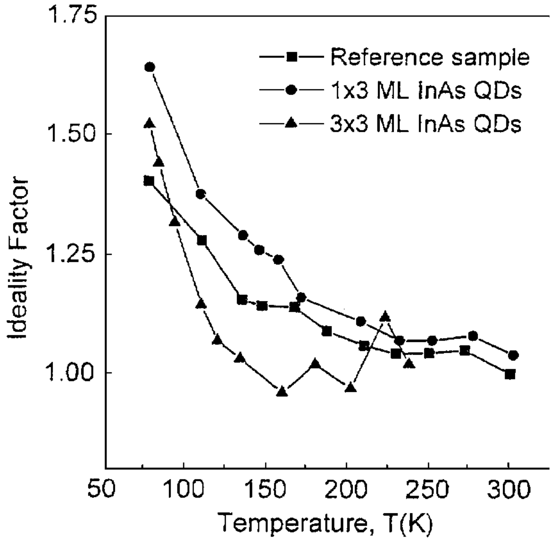

Figure 5. Variation of the ideality factor with temperature for the three types of Au/n-GaAs Schottky diodes.

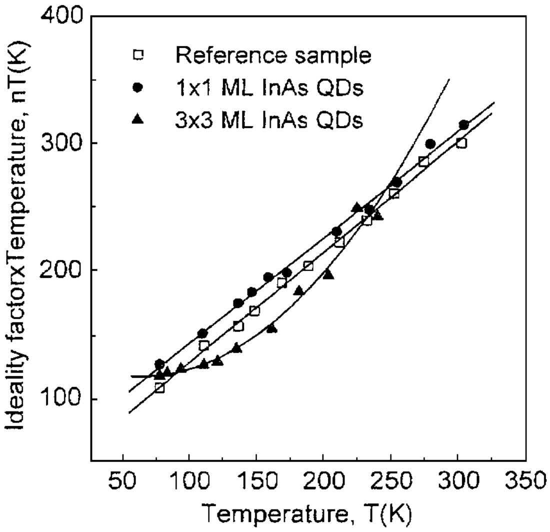

Figure 7. Plots of nT versus T with temperature for the three types of Au/n-GaAs Schottky diodes.

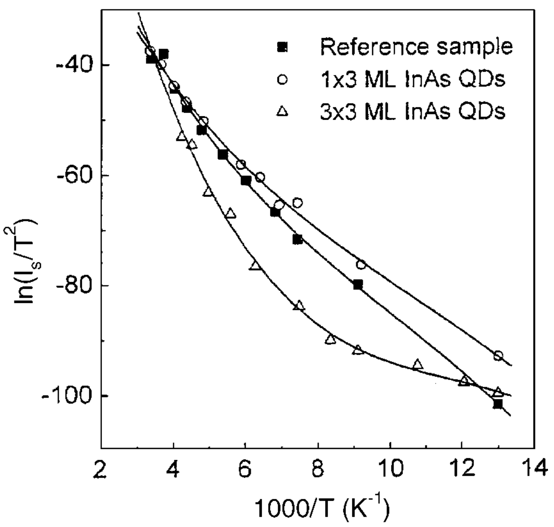

Figure 6. Richardson plots, $\ln(I_s/T^2)$ versus $1000/T$, obtained from the data of figure 3 with temperature for the three types of Au/n-GaAs Schottky diodes.

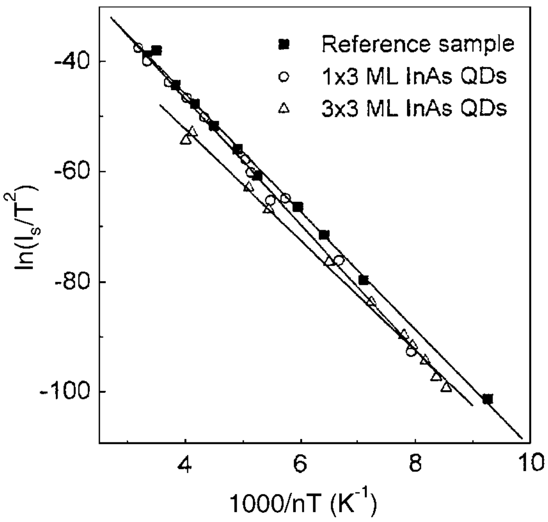

Figure 8. Modified Richardson plots, $\ln(I_s/T^2)$ versus $1000/nT$, obtained for the three types of Au/n-GaAs Schottky diodes.

with temperature is given by

$$n = 1 + \frac{T_0}{T} \tag{4}$$

where T_0 is a constant. The T_0-effect is usually demonstrated by plotting nT versus T and observing a straight line with a slope of unity which is not extrapolated through the origin of the axes. Figure 7 shows plots of nT versus T for the three types of investigated diodes. Straight lines with slopes of about 0.95 are observed for the reference diode and the diode containing one layer of InAs QDs with T_0 values 41 and 59.5 K, respectively. Tung [20] has demonstrated that as the temperature is lowered, SBH inhomogeneity leads to the T_0-effect. In an inhomogeneous Schottky barrier diode with a wide distribution of low SBH regions, theoretical calculations have shown that the ideality factor may increase at a rate even faster than the T_0-effect when the temperature is lowered [20]. This effect is significantly magnified when the series resistance R_s influences the current flowing through the low SBH regions [20]. Such a behaviour is observed for the Au/n-GaAs Schottky diode containing three layers of InAs QDs, characterized by large series resistance, as shown in figure 7. In the usual T_0-analysis the ideality factor n, as given by equation (4), is introduced into the denominator of the argument of the exponential function in the expression for the saturation current (equation (2)). When this is done with our data, the plots of $\ln(I_s/T^2)$ versus $1/nT$ give straight lines as shown in figure 8 for the three types of Au/n-GaAs Schottky diodes.

The anomalous behaviour observed in the *I–V* characteristics, such as the decrease of the SBH and the increase of the ideality factor with decreasing temperature and the nonlinearity in the Richardson plots, can be explained by adopting a continuous spatial distribution of the SBH approach. The variation of the barrier height over the contact area can be attributed to the charge modulation at the interface and QD planes. For the case of a Gaussian distribution of

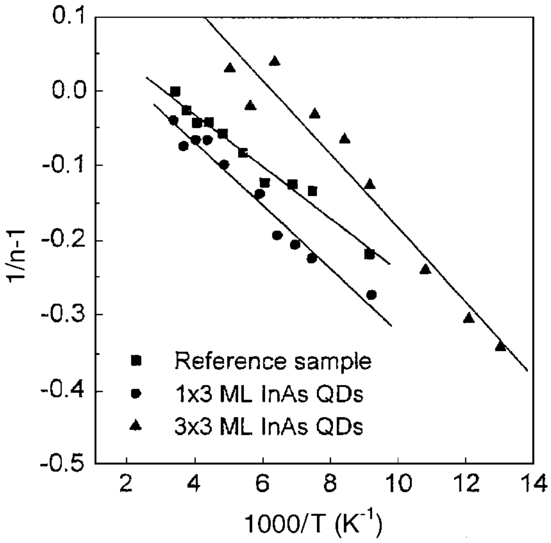

Figure 9. Plots of $1/n - 1$ versus $1000/T$ and linear fits for the three types of Au/n-GaAs Schottky diodes.

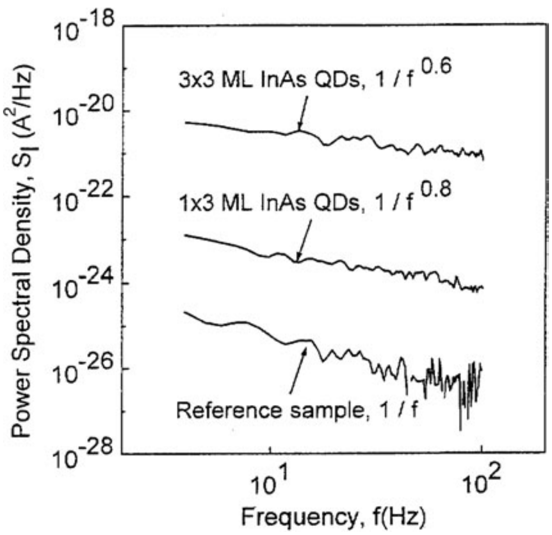

Figure 10. Typical spectral current density as a function of frequency for the three types of Au/n-GaAs Schottky diodes, measured at room temperature and bias current $I_F = 1 \times 10^{-7}$ A.

barrier height, the mean barrier height $\bar{\varphi}_b$ and the standard deviation of the barrier distribution σ are assumed to vary linearly with bias, i.e. $\bar{\varphi}_b = \bar{\varphi}_{b0} + \rho V$ and $\sigma = \sigma_0 + \xi V$, where $\bar{\varphi}_{b0}$ and σ_0 are the mean barrier height and standard deviation at zero bias and ρ, ξ are their voltage coefficients. The Gaussian distribution of the SBH yields the following equation for the barrier height [25, 26]:

$$\varphi_{b0} = \bar{\varphi}_{b0} - \frac{q\sigma_0^2}{2kT} \tag{5}$$

where $\bar{\varphi}_{b0}$ is the mean SBH at zero bias and extrapolated towards zero temperature and σ_0 is the standard deviation of the SBH distribution. The zero-bias barrier height has been simulated using equation (5) and replotted along the experimental values of φ_{b0} in figure 4 for the three types of Au/n-GaAs Schottky diodes. From the experimental and simulated barrier heights, one can see that there is very good agreement between these two values. This finding indicates that a Gaussian distribution of the barrier height over the contact area, arising from modulation of the charge at both interface and QD planes, is adequate to explain our experimental data. For the reference sample, we obtained the standard deviation for the Gaussian distribution of $\sigma_0 =$ 65 mV, whereas σ_0 increases to 70 mV in diodes containing one layer of InAs QDs. An increase in the number of QD layers to three layers, results in a further increase of the standard deviation to 90 mV.

According to the Gaussian fluctuation model [26], the variation of the ideality factor with temperature is given by

$$\frac{1}{n} = 1 - \rho + \frac{q\xi\sigma_0}{kT}. \tag{6}$$

The temperature dependence of the ideality factor can be understood on the basis of equation (6), which indicates that the plots of $1/n - 1$ versus $1/T$ should give straight lines with intercepts with y-axis and slopes dependent on the voltage coefficients ρ and ξ, respectively, as shown in figure 9 for the studied Schottky diodes. Using least-squares fitting to the experimental data of figure 9, we obtained the voltage coefficients $\rho = -0.11$ and $\xi = -0.03$ for the reference diode, $\rho = -0.1$ and $\xi = -0.06$ for the diode containing one layer of InAs QDs and $\rho = -0.31$ and $\xi = -0.07$ for the diode containing three layers of InAs QDs. These results reveal that the bias voltage homogenizes the barrier height fluctuation, i.e. as the bias voltage increases the barrier height distribution becomes narrower since $\sigma = \sigma_0 + \xi V$ and $\xi < 0$. This has been explained by the image force shift of the effective barrier maximum deeper into the semiconductor when the bias voltage increases, thus homogenizing the SBH distribution [21]. The SBH homogenization affects the noise behaviour as will be discussed later.

3.2. *Low frequency noise characteristics*

Figure 10 shows typical current noise spectra of the studied diodes at room temperature and bias current $I_F = 10^{-7}$ A. The current noise spectral density S_I at constant frequency ($f =$ 10 Hz) as a function of the forward current I_F is shown in figure 11 for the three diodes. The noise measurements were restricted in the current regions where there is no influence of the series resistance on the current noise. The reference diode shows $1/f$ noise dependence over a wide frequency range and the $1/f$ noise level scales with I_F^2 as shown in figures 10 and 11, respectively. In this diode, we attribute the origin of the $1/f$ noise to modulation of the Schottky barrier due to trapping and detrapping processes in interface traps uniformly distributed in energy [27]. Considering that the current fluctuation is due to the random walk of electrons at the Au/n-GaAs interface via modulation of the barrier height, the noise intensity is related to the interface states density D_{it} by the relationship [27]

$$S_I(f) = \frac{G}{f}\left(\frac{qI_F}{4\varepsilon}\right)^2 \frac{q^2 D_{it}}{\pi kT N_d W A} \tag{7}$$

where the constant G has the value of 0.1, ε is the permittivity of the semiconductor, N_d is the doping concentration of the n-type semiconductor and W is the width of the depletion region of the contact. For the reference diode, the current dependence

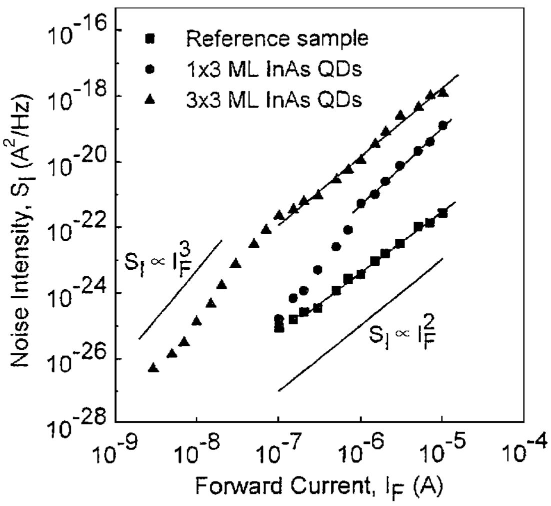

Figure 11. Noise power density S_I as a function of the forward bias current I_F for the three types of Au/n-GaAs Schottky diodes, measured at room temperature and frequency $f = 10$ Hz.

of S_I is linear with a slope close to 2 (figure 11) and the noise intensity can be explained by the random walk model (equation (7)) with an interface state density $D_{it} = 3 \times 10^{11}$ cm^{-2} eV^{-1}.

In the case of the Schottky diodes containing layers of InAs QDs, the noise spectra exhibit $1/f^\gamma$ (with $\gamma < 1$) behaviour as shown in figure 10. The $1/f^\gamma$ noise level scales with I_F^3 in the range of low currents, whereas at higher currents S_I varies linearly with a slope close to 2. It is clearly observed that the noise intensity is higher by about one order of magnitude in the diode containing three layers of InAs QDs. This finding indicates that as the number of incorporated InAs QD layers increases, the QD-induced trap density increases. The $1/f^\gamma$ (with $\gamma < 1$) spectra indicate that the noise originates from fluctuation in the carrier number due to trapping–detrapping processes in traps with an exponential energy distribution in the depletion region of the contacts [28]. For the exponential trap distribution

$$N_t(E) = N_0 \exp\left(\frac{E - E_c}{E_0}\right) \quad (8)$$

where E and E_c are the trap energy level and the conduction band-edge energy and N_0, E_0 are the distribution parameters, the noise intensity is given by [28]

$$S_I = \left(\frac{q^2 I_F}{4\varepsilon}\right)^2 \frac{N_0}{N_d} \frac{1}{2qA(V_D - V)} \frac{\tau_0^{1-\gamma}}{\sin(\gamma\pi/2)} \frac{1}{(2\pi f)^\gamma} \quad (9)$$

where V_D is the diffusion potential of the Schottky contact and $\tau_0 = 10^{-12}$ s is the inverse of the 'attempt to escape' frequency. The frequency exponent γ is related to the trap distribution parameter E_0 according to [28]

$$\gamma = 1 - \frac{kT}{E_0}. \quad (10)$$

In the range of high forward currents, S_I is proportional to I_F^2 for the diodes containing InAs QDs as shown in figure 11, in agreement with equation (9). The quadratic S_I dependence over a wide range of currents suggests that the Schottky diodes are homogeneous in barrier height [29], in agreement with the conclusion obtained from the current transport data in the high bias voltage range. In the range of low forward currents, the faster increase of S_I with increasing I_F (figure 11) can be explained by considering that the forward current is dominated by the current passing through small circular patches of reduced SBH with an effective area [20]:

$$A_{\text{eff}} = \frac{4\pi\gamma_0 kT}{9q\alpha_0^2(V)} \quad (11)$$

and

$$\alpha_0(V) = \left[\frac{qN_d}{\varepsilon}(\varphi_{b0} - V_D - (V - IR_s))\right]^{1/3} \quad (12)$$

where the circular inhomogeneities are characterized by the parameter $\gamma_0 = 3(R_p^2\Delta_p/4)^{1/3}$, i.e. by the product of the patch area πR_p^2 and the deviation Δ_p of their local barrier height from the homogeneous value φ_{b0}. Equations (11) and (12) reveal that the low SBH patch is characterized by an effective area (A_{eff}) which is bias dependent, i.e. A_{eff} is decreased as the bias voltage V is increased. Since the noise intensity is inversely proportional to the area where the noise sources are located, the decrease of A_{eff} with increasing V is reflected as a current dependence for the noise intensity of the form $S_I \propto I_F^n$ with $n > 2$.

From the noise data of figure 11 lying in the current range where $S_I \propto I_F^2$ holds, using equation (9) we can determine the trap distribution parameter N_0, whereas from the frequency exponent γ we can determine the distribution parameter E_0 using equation (10). From the data of figures 10 and 11 we determined the trap parameters $E_0 = 64.6$ meV, $N_0 = 6.8 \times 10^{20}$ cm^{-3} eV^{-1} and $E_0 = 130$ meV, $N_0 = 2.3 \times 10^{22}$ cm^{-3} eV^{-1} for the diodes containing one or three layers of InAs QDs, respectively. The larger values of N_0 and E_0 in the Schottky diode containing three layers of QDs results in deep tails in the forbidden gap of higher density, indicating that the degree of disorder of the GaAs material increases as the number of incorporated layers of InAs QDs is increased. Thus, the noise data indicate that distortion of the bonds occurs in the capping GaAs layer due to QD formation, which results in the generation of exponential band tail states.

4. Conclusions

The forward current–voltage characteristics of Au/n-GaAs Schottky diodes, with embedded one or three layers of InAs QDs, were studied in the temperature range of 77–300 K. The zero-bias barrier height decreases and the ideality factor increases with decreasing temperature. The ideality factor was found to show the T_0-effect and the curved Richardson plots were linearized after applying the T_0-analysis. These findings were successfully explained on the basis of the thermionic-emission diffusion mechanism by incorporating the concept of barrier height inhomogeneity, which is described as a Gaussian distribution over the contact area. In the diode containing layers of InAs QDs, an excess current is observed at low bias voltages, attributed to the contribution of small patches of lowered Schottky barrier height.

In the reference Schottky diode, the power spectral density of the current fluctuations shows $1/f$ behaviour and is proportional to I_F^2. These data were explained by the random walk model based on the barrier height modulation due to trapping–detrapping processes of carriers in interface states of density $D_{it} = 3 \times 10^{11}$ cm^{-2} eV^{-1}. In Schottky diodes containing layers of InAs QDs, at low currents the noise intensity increases fast with current following a law of the form $S_I \propto I_F^3$, attributed to the bias dependence of the effective area of small patches of reduced barrier height in the Schottky area. In the high current range, S_I shows $1/f^{\gamma}$ (with $\gamma < 1$) behaviour and follows the quadratic current dependence law. These data were explained by fluctuation in the number of carriers due to trapping–detrapping processes in traps with exponential energy distribution, generated in the depletion region of the contact due to the QD formation.

Acknowledgments

The authors N A Hastas, D H Tassis and C A Dimitriadis thank the Greek General Secreteriat of Research and Technology for financial support within the frame of bilateral R&D cooperation between Greece and Hungary.

References

[1] Bimberg D, Grundmann M and Ledentsov N N 1998 *Quantum Dot Heterostructures* (Chichester: Wiley)
[2] Leonard D, Pond K and Petroff P M 1994 *Phys. Rev.* B **50** 11687
[3] Drexler H, Leonard D, Hansen W, Kotthaus J P and Petroff P M 1994 *Phys. Rev. Lett.* **73** 2252
[4] Kaptyen C M A, Heinrichsdorff F, Stier O, Heitz R, Grundmann M, Zakharov N D and Bimberg D 1999 *Phys. Rev.* B **60** 14265
[5] Campbell J C, Huffaker D L and Deng H 1997 *Electron. Lett.* **33** 1337
[6] Arakawa Y and Sakaki H 1982 *Appl. Phys. Lett.* **40** 939
[7] Heinrichsdorff F, Mao M-H and Kirstaedter N 1997 *Appl. Phys. Lett.* **71** 22
[8] Yusa G and Sakaki H 1997 *J. Appl. Phys.* **70** 345
[9] Finley J J, Skalitz M, Arzberger M, Zrenner A, Bohm G and Abstreiter G 1998 *Appl. Phys. Lett.* **73** 2618
[10] Henini M, Bronnkov P N, Polimeni A, Stoddart S T, Main P C, Eaves L, Kovsh A R, Musiklin Yu G and Konnikov S G 1999 *Superlattices Microstruct.* **25** 105
[11] Horvath Zs J, Dozsa L, Van Tuyen Vo, Podor B, Nemcsics A, Frigeri P, Gombia E, Mosca R and Franchi S 2000 *Thin Solid Films* **367** 89
[12] Dozsa L, Horvath Zs J, Van Tuyen Vo, Podor B, Mohacsy T, Franchi S, Frigeri P, Gombia E and Mosca R 2000 *Microelectron. Eng.* **51–52** 85
[13] Wang H L, Ning D, Zhu H J, Chen F, Wang H, Wang X D and Feng S L 2000 *J. Cryst. Growth* **208** 107
[14] Horvath Zs J, Frigeri P, Franchi S, Van Tuyen Vo, Gombia E, Mosca R and Dozsa L 2002 *Appl. Surf. Sci.* **190** 218
[15] Vandamme L K J 1994 *IEEE Trans. Electron Devices* **41** 2176
[16] Hastas N A, Dimitriadis C A, Dozsa L, Gombia E, Amighetti S and Frigeri P 2003 *J. Appl. Phys.* **93** 3990
[17] Hastas N A, Dimitriadis C A, Dozsa L, Gombia E and Mosca R 2003 *J. Appl. Phys.* **93** 5833
[18] Bosacchi A, Frigeri P, Franchi S, Allegri P and Avanzini V 1997 *J. Cryst. Growth* **175–176** 771
[19] Rhoderick E H and Williams R H 1988 *Metal-Semiconductor Contacts* 2nd edn (Oxford: Clarendon)
[20] Tung R T 1992 *Phys. Rev.* B **45** 13509
[21] Zhu S, Van Meirhaeghe R L, Detavernier C, Cardon F, Ru G-P, Qu X-P and Li B-Z 2000 *Solid-State Electron.* **44** 663
[22] Sze S M 1981 *Physics of Semiconductor Devices* 2nd edn (New York: Wiley)
[23] Levine J D 1971 *J. Appl. Phys.* **42** 3991
[24] Crowell C R 1977 *Solid-State Electron.* **20** 171
[25] Song Y P, Vanmeirhaeghe R L, Laflere W H and Cardon F 1986 *Solid-State Electron.* **29** 633
[26] Werner J H and Guttler H H 1991 *J. Appl. Phys.* **69** 1522
[27] Lee J I, Brini J, Chovet A and Dimitriadis C A 1999 *Solid-State Electron.* **43** 2185
[28] Lee J I, Brini J, Chovet A and Dimitriadis C A 1999 *Solid-State Electron.* **43** 2181
[29] Papatzika S, Hastas N A, Angelis C T, Dimitriadis C A, Kamarinos G and Lee J I 2002 *Appl. Phys. Lett.* **80** 1468